PHILOSOPHICAL TRANSACTIONS OF THE ROYAL SOCIETY A MATHEMATICAL, PHYSICAL & ENGINEERING SCIENCES

Oscillatory Ignitions and Cool Flames in the Oxidation of Butane in a Jet-Stirred Reactor

V. K. Proudler, P. Cederbalk, A. Horowitz, K. J. Hughes and M. J. Pilling

Phil. Trans. R. Soc. Lond. A 1991 **337**, 211-221
doi: 10.1098/rsta.1991.0118

Oscillatory ignitions and cool flames in the oxidation of butane in a jet-stirred reactor

By V. K. Proudler, P. Cederbalk†, A. Horowitz‡, K. J. Hughes and M. J. Pilling

School of Chemistry, University of Leeds, Leeds LS2 9JT, U.K. and Physical Chemistry Laboratory, South Parks Road, Oxford OX1 3QZ, U.K.

The oxidation of butane ($[C_4H_{10}]:[O_2] = 1.13:1.00$) has been studied over the temperature and pressure ranges $371 \leqslant T/\mathrm{K} \leqslant 675$, $226 \leqslant P/\mathrm{Torr} \leqslant 489$ in a jet stirred reactor with a residence time of 9.4 s (1 Torr $\approx$ 133.3 Pa). The gas temperature and pressure were probed and phase diagrams constructed delineating regions of oscillatory ignitions and cool flames, and high- and low-temperature stationary states. On heating at an initial pressure of 400 Torr from 570 K sharp transitions were observed, first to an oscillatory ignition and then to an oscillatory cool flame region, followed by a smooth transition to a high-temperature stationary state via a supercritical Hopf bifurcation. On cooling from this high-temperature stationary state, oscillatory cool flames were observed with a sharp extinction at 542 K, without any entry to the oscillatory ignition region. The latter could be entered, however, by suddenly cooling the system from the oscillatory cool flame region by temporarily substituting nitrogen for oxygen in the gas streams. Complex waveforms, consisting of bursts of oscillatory cool flames interspersed with periods of monotonic cooling, were also observed at lower pressures. A Nd:YAG pumped dye laser was used to probe laser induced fluorescence from formaldehyde in the oscillatory ignition region. Variations in the internal surface of the reactor demonstrated the significance of surface reactions. An outline mechanism, based on detailed numerical simulations, is presented to account for the shape of the ignition profiles and the transition from multiple ignitions to oscillatory cool flames.

1. Introduction

Studies of gas phase oxidation in continuous stirred tank reactors (CSTR) have provided an ideal vehicle for the development of an understanding of the thermokinetic mechanisms underlying oscillatory reactions. Gray & Scott (1991) recently reviewed the experimental results from studies of $H_2 + O_2$, $CO + H_2 + O_2$ and $CH_3CHO + O_2$ in a CSTR and provided a theoretical framework for these results based primarily on simple analytic models.

The low temperature oxidation of hydrocarbons, where oscillatory behaviour has also been observed (Caprio *et al.* 1976, 1981, 1983), is of significance in autoignition in spark ignition engines. There is a need to understand, in detail, the chemical mechanism of autoignition and to develop methods for reducing such mechanisms for incorporation in computational fluid dynamic codes. Experimental validation is a

† Permanent address: Lund Institute of Technology, Combustion Centre, Box 118, 5-22100 Lund, Sweden.
‡ Permanent address: Soreq Nuclear Research Centre, Yavne, Israel.

Phil. Trans R. Soc. Lond. A (1991) **337**, 211–221
Printed in Great Britain

vital stage in model development as illustrated by the recent work Olsson & Cox (1991) who tested their detailed numerical model for butane oxidation on the rapid compression experiments of Franck *et al.* (1988) and Griffiths *et al.* (1988). The present experiments represent a further attempt to provide experimental validation for that model, while, at the same time, examining the range of thermokinetic phenomena displayed by this system in a CSTR.

2. Experimental

The optimal design of a well-mixed jet stirred rector has been calculated and tested experimentally by Bush (1969) and the reactor used in this work (figure 1) was a stainless steel cylinder, approximating to the toroidal shape examined by Bush. A Pyrex or quartz liner was used to avoid contact of the reacting gas mixture with the metal surface. The internal height of the lined reactor was equal to its diameter (8.6 cm), giving a total volume of 500 cm^3. The jets were constructed from 0.6 cm stainless steel tubing and had diameters of 0.04 cm. Four jets were used in total, at two levels of height 2.15 and 6.45 cm in the reactor and at a distance of 4.3 cm from the centre; the jets at the two levels were offset by 90° (figure 1) and Bush's optimal jet direction (an angle of 70° to the radius) was used. At a total pressure of 40 Torr and with a kinematic viscosity of 0.173 $cm^2\ s^{-1}$, Bush's design gives maximum and minimum flow rates for optimal mixing of 70 and 35 $cm^3\ s^{-1}$ respectively. In this work, a residence time of 9.4 ± 0.4 s (defined as the ratio of the reactor volume to the volumetric flow rate) was used for the initial conditions, which were varied over the range $371 \leqslant T/\mathrm{K} \leqslant 675$, $266 \leqslant P/\mathrm{Torr} \leqslant 489$. The maximum normalized mixing time, $\tau_{0.01}$, defined by Bush as the fraction of the residence time for which the concentration variations in the reactor are less than 1% of the average concentration was chosen as 0.3. This value limits the ratio of the jet diameter and the circumferential distance between the jets.

The reactor was constructed from a stainless steel cylinder with 2.75 cm thick walls. The base was welded to the cylinder, while the top of the reactor was removable and was sealed with a copper gasket. The outlet to the vacuum pumps was a 0.6 cm stainless steel tube in the centre of the base. The reactor was heated by four 500 W Watlow firerod cartridge heaters embedded in the reactor walls. A thermocoax Type K thermocouple, cemented to the outer wall of the reactor, acted as a sensor to the temperature controller which could hold the wall temperature constant or ramp it. A second Type K thermocouple was placed inside the reactor directly below one of the upper jets and near the horizontal plane of the lower jets. The system maintained the outer wall temperature to $^{+4}_{-2}$ K and the inner temperature to ± 1 K at a typical temperature of 600 K with a non-reactive gas mixture. The rapid temperature variations in reacting gas mixtures were monitored with a Pt–Pt/13% Rh thermocouple (Omega Engineering) with a tip constructed from 25 μm wire, giving an optimal response time of 70 ms, welded to 50 μm wire. The thermocouple was placed above one of the lower jets and near the plane of the upper jets (figure 1). Both uncoated and silica coated thermocouples were used and were calibrated against the internal type K thermocouple.

Four flow lines, two for *n*-butane and two for oxygen or nitrogen were used to feed gases to the four jets, using four Tylan FC260 mass flow controllers. The four supply lines were paired so that *n*-butane and oxygen (nitrogen) were each fed to an upper and lower jet. The flow controllers were calibrated for the specific gas used with

PHILOSOPHICAL TRANSACTIONS OF THE ROYAL SOCIETY A MATHEMATICAL, PHYSICAL & ENGINEERING SCIENCES

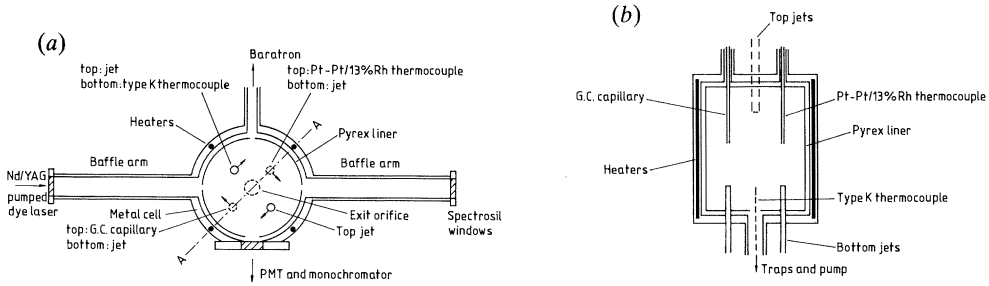

Figure 1. Diagram of the jet-stirred reactor. (*a*) Horizontal cross section, (*b*) vertical cross section along A–A.

bubble flow meters. A 1.8 m 700 W Hotfoil heating tape, insulated with ceramic wool (Kaowool), was wrapped around each pair of supply lines to preheat the gases. Type K thermocouples were used as sensors for the temperature controller and the supply lines were held within ± 3 K of the set temperature.

The exit port of the reaction cell was connected, via a Hoke needle valve and two Pyrex traps cooled to liquid nitrogen temperatures, to a two stage rotary pump (Edwards E1M5). A larger rotary pump (Edwards ED 330) was connected directly to the reactor via a large bore valve to provide more rapid pump out. The pressure in the reactor was monitored using a MKS 1000 Torr Baratron gauge, connected via a short 10 mm diameter stainless steel tube to minimize the response time.

The reactor was also probed using a frequency-doubled Nd:YAG pumped dye laser operating with Rhodamine 6G and providing output in the range 280–290 nm at a repetition rate of 25 Hz. The laser beam was passed into and out of the reactor via 0.5 m baffle arms and the resulting fluorescence was focussed on to the slit of an Applied Photophysics f/3.4 0.25 m monochrometer and detected using an EMI 9813 KB photomultiplier. The intensity of the laser beam was constantly monitored allowing the fluorescence intensity to be normalized. The signals were recorded using a sample and hold unit with 1μs gates, which was interfaced to a microcomputer. The temperature and pressure signals were also digitized and stored on the computer, with sampling intervals of from 1–100 ms.

The *n*-butane was BOC pure grade N2.0 (greater than 99.0% pure, impurities *i*-butane, *i*-pentane, *n*-pentane), the oxygen was greater than 99.5% pure and the nitrogen greater than 99.998% pure.

3. Results

n-Butane and nitrogen were flowed through the reactor and, when the temperature was stable, the experiment was initiated by switching from nitrogen to oxygen. A volume flow rate ratio of 1.13:1.0 (*n*-butane:oxygen) was used, with a total flow rate of 830 sccm and an initial mean residence time of (9.4 ± 0.4) s. Experiments could be conducted either at constant or ramped wall temperature. In the initial experiments, the initial pressure was held fixed at 400 Torr and the effects of increasing the cell temperature from 570 K were studied. There were significant variations in the pressure during the experiments; some examples are reported below.

PHILOSOPHICAL TRANSACTIONS OF THE ROYAL SOCIETY A MATHEMATICAL, PHYSICAL & ENGINEERING SCIENCES

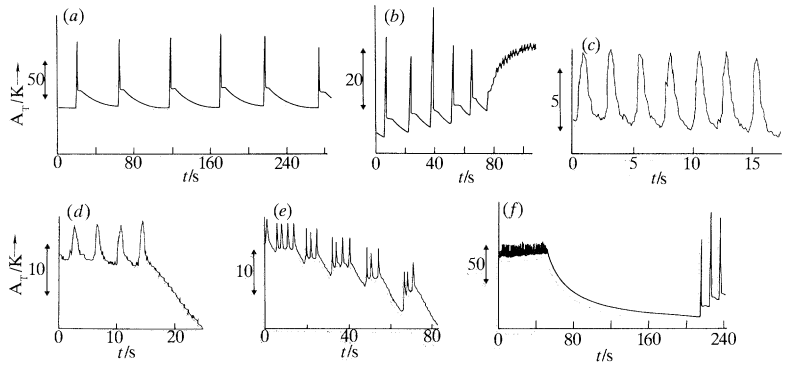

Figure 2. Temperature profiles for an initial temperature of 570 K. Unless otherwise stated, the initial pressure was 400 Torr. (*a*) Oscillatory ignitions, $T_{wall} = 577$ K; (*b*) transition from oscillatory ignitions to oscillatory cool flames, $T_{wall} = 579$ K; (*c*) oscillatory cool flames, $T_{wall} = 579$ K; (*d*) cessation of cool flames on cooling, $T_{wall} = 542$ K; (*e*) repeated re-ignition of cool flames on cooling ($T_{wall} = 542$ K, initial pressure = 300 Torr); (*f*) perturbation of oscillatory cool flames to generate oscillatory ignitions on cooling (see text).

(*a*) *Heating experiments*

(i) *Low-temperature steady state*

At temperatures below 579 K, a steady-state reaction régime was observed, with no detectable light emission. The temperature excess ($T_{gas} - T_{wall}$) was small, typically less than 10 K.

(ii) *Oscillatory ignitions*

A transition was observed at $T_{wall} = 579$ K ($T_{gas} = 596$ K) to an oscillatory ignition region. Although the response at 579 K was not completely stable at $T_{wall} = 579$ K (see (iii) below), once this region was located the oscillatory ignitions could be maintained by reducing the wall temperature. The characteristic set of temperature and pressure profiles shown in figure 2*a* refers to a wall temperature of 577 K; the frequency, ν, is (0.021 ± 0.006) Hz, where the uncertainty refers to two standard deviations. The oscillations in temperature and pressure were in phase within the resolution of the experiment (less than 0.1 s) and the recorded temperature and pressure excursions, ($A_T(\max) = T_{gas}(\max) - T_{gas}(\min)$ and $A_p(\max) = P_{gas}(\max) - P_{gas}(\min)$) were $A_T(\max) = (51.0 \pm 1.7)$ K and $A_P(\max) = (191.0 \pm 7.2)$ Torr. The former, in particular, is likely to be an underestimate of the true temperature rise, because of the limited time response of the thermocouple. The ignitions correspond to relaxation oscillations with a characteristic tail.

(iii) *Transition to cool flames*

On increasing T_{wall} to 579 K a transition was observed from oscillatory ignitions to cool flames, which had the nature of a slow evolution of the waveform, followed by an abrupt change. With T_{wall} held fixed at the transition temperature, the amplitude of the ignitions decreased, whereas the temperature minimum between the excursions increased (figure 2*b*). Following a sudden jump in temperature, the system eventually settled to a response with much smaller oscillations about a higher gas temperature.

The same transition behaviour was observed whether the oscillatory ignition region was entered transiently at $T_{wall} = 579$ K, on heating from the low-temperature

stationary state (see above), or was maintained by cooling from 579 K to 577 K, with subsequent reheating to the transition temperature.

(iv) *Oscillatory cool flames*

The stable oscillations observed in the cool flame region were of smaller amplitude than the ignitions and were approximately sinusoidal. Figure 2*c* shows a typical example, at $T_{\text{wall}} = 579$ K ($T_{\text{gas}} = 625$ K) with $A_{\text{T}}(\text{max}) = (7.2 \pm 0.8)$ K, $A_{\text{P}}(\text{max}) = (11.9 \pm 2.9)$Torr and $\nu = (0.57 \pm 0.06)$ Hz. On increasing the wall temperature, the amplitude of the oscillations decreased, slowly at first, and their frequency increased. Eventually, at $T_{\text{wall}} = 581$ K ($T_{\text{gas}} = 640$–647 K), the amplitude became infinitesimally small and the system entered a new steady-state region.

(v) *High-temperature steady state*

The high-temperature steady state was associated with a temperature excess of approximately 100 K and with rapid reaction, as determined in separate end product analysis experiments.

(*b*) *Cooling experiments*

(i) *Gradual cooling*

On cooling from the high-temperature steady state, the oscillatory cool flame region was re-entered. The amplitude of the oscillations gradually increased and the frequency decreased as the wall temperature was reduced until at $T_{\text{wall}} = 542$ K ($T_{\text{gas}} = 618$ K) the oscillations were suddenly extinguished (figure 2*d*) and the gas temperature fell rapidly as the system entered the lower steady-state mode.

The oscillatory ignition region was not entered spontaneously during this cooling period but, as described above, stable oscillatory ignitions could be generated by cooling from 579 K to 577 K once they had been established in the heating cycle. Further cooling from 577 K led to a gradual decrease in the frequency of the multiple ignitions until the period became immeasurably long at $T_{\text{wall}} = 569$ K.

(ii) *Perturbation experiments*

Although oscillatory ignitions were not observed on gradual cooling from the high-temperature steady state, they could be generated by perturbing the oscillatory cool flames in the cooling cycle at temperatures between 579 K and 569 K. Figure 2*f* shows the effects of switching from oxygen to nitrogen in the oscillatory cool flame region at a wall temperature of 577 K. T_{gas} fell rapidly and, on switching back to oxygen, oscillatory ignitions were observed.

(*c*) *Effects of pressure*

The effects of pressure on the sequences described above are conveniently summarized on pressure/temperature phase diagrams. Figure 3 shows the starting-pressure/wall-temperature plane and maps out the transitions between the various thermokinetic phenomena as a function of imposed conditions. The transitions were very sensitive to T_{wall} in the heating experiments and occurred over a very small range of wall temperatures; in consequence all the transitions are precisely located in figure 3. The diagram also demonstrates the significant hysteresis effects, with considerable reductions in the transition temperatures on cooling.

It is also instructive to construct a phase diagram based on T_{gas} and the recorded pressure which is shown in figure 4. For oscillatory responses, T_{gas} and P_{gas} are taken as the minimum temperature and pressure during the excursions. As discussed

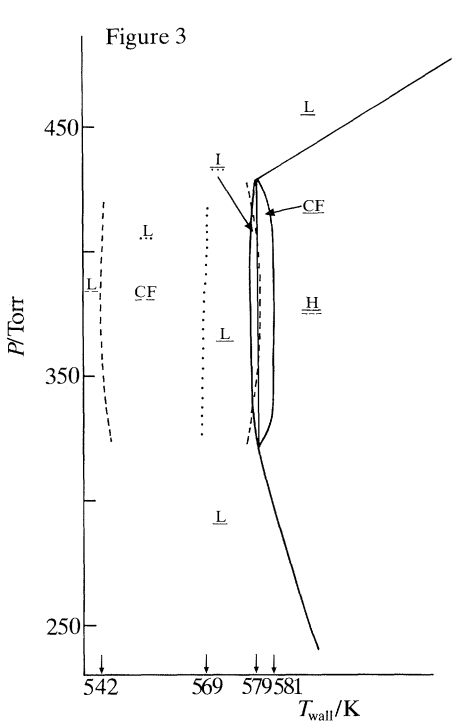

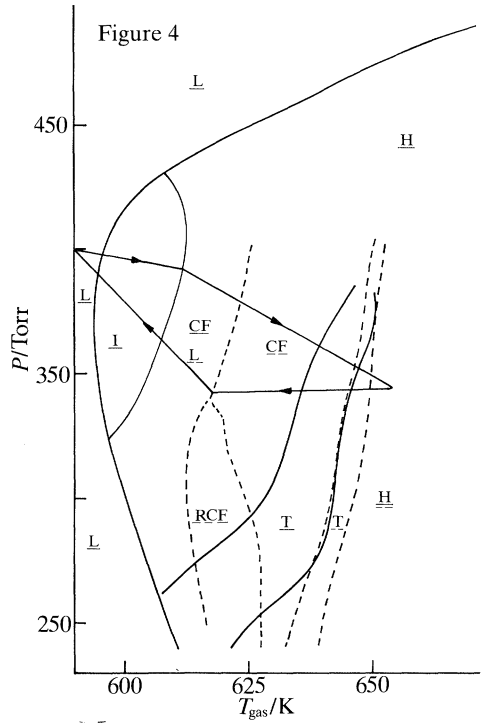

Figure 3. Pressure wall-temperature phase diagram. The full lines are for heating, the dashed lines for cooling, from H, and the dotted line for cooling from I. L, low-temperature steady state; I, ignitions; CF, cool flames; H, high-temperature steady state

Figure 4. Initial pressure: gas temperature phase diagram. The full lines are for the heating phase of the cycle, the dashed lines for cooling from the high-temperature steady state: L, low-temperature steady state; I, ignitions; CF, cool flames; H, high-temperature steady state; RCF, repeated re-ignition of cool flames; T, transition regions from CF ↔ H. A typical trajectory is shown by the arrowed cycle.

above, the cool-flame/high-temperature transitions were smooth and continuous and can only be indicated as a transition region; all other transitions were sharp and can be precisely located.

Figure 4 also shows a typical trajectory for an initial pressure of 400 Torr. On increasing the temperature, the pressure fell slowly in both the low-temperature steady state and oscillatory ignition regions. On entering the oscillatory cool flame region, however, a more rapid decrease in pressure was observed which continued into the high-temperature steady-state region. On cooling, the trajectory was not simply reversed, but the pressure remained low until the oscillatory cool flames were suddenly extinguished when further cooling led to an increase in pressure until the initial pressure-temperature conditions were re-established.

Figure 4 also demonstrates a new region only observed on cooling at lower initial pressures (250–300 Torr), which is illustrated in figure 2*e*. On cooling from the high-temperature steady state, oscillatory cool flames were observed, but at the lower end of the range a bursting pattern corresponding to repeated re-ignition of cool flame oscillations was observed. The slow decrease in the wall temperature was accompanied by a slow decrease in the background gas temperature. Eventually the cool flames were extinguished and T_{gas} fell more rapidly followed by a spontaneous

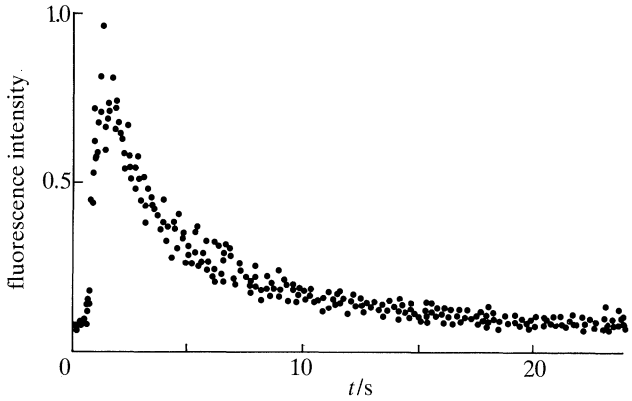

Figure 5. Averaged normalized fluorescence intensity at 322 nm following laser excitation at 288.7 nm. The data are averaged over 32 ignitions. $T_{\text{wall}} = 577$ K; $P_{\text{initial}} = 400$ Torr.

re-ignition. The newly established background gas temperature was lower than that observed in the previous cycle of cool flames. As the wall temperature continued to fall, the re-ignition cycle was repeated several times until T_{gas} fell to *ca.* 614 K when no further re-ignitions were observed.

(*d*) *Surface effects*

Both quartz and Pyrex liners were used and also a Pyrex liner coated with silica. The temperature excursions were greater for the quartz and silica coated surfaces for both the multiple ignitions and the cool flames and the shapes of the cool flames were much less regular than those observed with a Pyrex liner. All the results described above were obtained with a Pyrex liner.

(*e*) *Laser induced fluorescence* (LIF) *studies*

Initial experiments were designed to eliminate interferences from the butane Raman signal. With the laser tuned to 282.33 nm, corresponding to the $Q_1(3)$ line of OH $[A^2\Sigma^+(v' = 1) - X^2\Pi(v'' = 0)]$ a low pressure (< 1 Torr) of HNO_2 was placed in the cell. OH fluorescence was observed at *ca.* 316 nm $(A(v' = 1) - X(v'' = 1))$. Addition of 64 Torr of butane produced a substantial signal due to Raman scattering at *ca.* 308 nm, with a tail extending into the OH (1,1) band. Interference from the scattered signal was minimized by observing OH at wavelengths to the red of the 316 nm maximum.

Figure 5 shows a plot of the intensity of the fluorescence obtained by averaging over 32 ignition pulses, with a laser frequency of 25 Hz. The fluorescence pulses were normalized to the frequency doubled dye laser intensity. The intensity at the peak varied linearly with laser intensity, demonstrating that a single photon process was responsible for generating the fluorescence.

Tuning the laser to 288.7 nm, where OH does not absorb, led to behaviour identical to that reported above and scanning the monochromater to longer wavelengths showed a broad emission spectrum extending up to 350 nm. These observations are most readily rationalized by ascribing the absorbing species to formaldehyde, although some contribution may also be made by OH for $\lambda_{\text{ex}} = 282.33$ nm. No change was discernible in the shape of the fluorescence ignition peaks on changing the wavelength.

Finally, we note that the fluorescence ignition profiles were in phase with the temperature profiles and that the decay of fluorescence was biexponential (figure 5) with half-lives of 2.5 s and 14 s.

4. Discussion

The behaviour of an equimolar butane, oxygen mixture has been studied previously in a paddle stirred reactor as a function of residence time (10–35 s) by Caprio *et al.* (1983). Behaviour similar to that reported here was observed, including multiple ignitions, oscillatory cool flames, hysteresis and multistability. Although the initial pressure and temperature were not varied for a constant residence time, Caprio *et al.* constructed a T_{gas}/residence-time phase diagram which complements the P_{gas}/T_{gas} and P/T_{wall} phase diagram presented here. The observations of repeated re-ignition of cool flames on reducing T_{wall}, of the stabilization of the multiple ignitions on reducing T_{wall} and of the perturbation of the oscillating cool flames to generate multiple ignitions are novel for this system. More limited studies of butane oxidation in a CSTR have also been made by Ferrer *et al.* (1983), while multiple cool flames and two stage ignition have been observed in static reactors (Malherbe & Walsh 1950; Bardwell 1954; Neu 1956). These experiments have been reviewed in some detail by Griffiths (1986).

Pugh *et al.* (1987) have reported LIF studies of OH during oscillatory ignitions and cool flames in the oxidation of ethanal where OH was found to be in phase with oscillations in [CH_3CHO], temperature, pressure and chemiluminescence intensity. Baulch *et al.* (1990) monitored OH in H_2/O_2 in a jet stirred reactor by resonance absorption demonstrating that the signals were in phase with the temperature although the latter showed a slower decay. More recently, as discussed in Baulch *et al.* (1991), H has been probed in the same system using resonance enhanced multiple photon ionization.

The reaction patterns observed for other fuel/oxygen systems have been discussed by Gray & Scott (1990) on the basis of model reaction schemes. The behaviour may be rationalized using a bifurcation diagram, which must accommodate the sudden transition from a lower-temperature steady state to oscillatory ignition and then to oscillatory cool flame regions, followed by a smooth transition to a high-temperature steady state. The overlap of the two types of oscillatory behaviour, and the dependence of their accessibility on the previous history of the experiment, together with the hysteresis shown in the transition temperatures, is an example of bihythmicity arising from the coexistence of two stable limit cycles with large and small amplitudes.

A bifurcation diagram, which displays the necessary features, is shown in figure 6. On increasing the temperature, the lowest stationary-state locus is followed until $T_{wall} = 579$ K, when this state becomes unstable and a transition in which the system passes close to a large amplitude limit cycle occurs which itself becomes unstable at this temperature, giving way to a small-amplitude, high-frequency limit cycle, corresponding to the oscillatory cool flames. Increasing the temperature leads to a decrease in amplitude of the cool flames and to a smooth transition at 581 K to the high-temperature stationary state via a supercritical Hopf bifurcation.

On decreasing the temperature, the system stays in the small amplitude limit cycle until stability is lost at 542 K. The high-amplitude limit cycle can be reached by heating to 579 K followed by cooling before the transition to the oscillatory cool

PHILOSOPHICAL TRANSACTIONS OF THE ROYAL SOCIETY A MATHEMATICAL, PHYSICAL & ENGINEERING SCIENCES

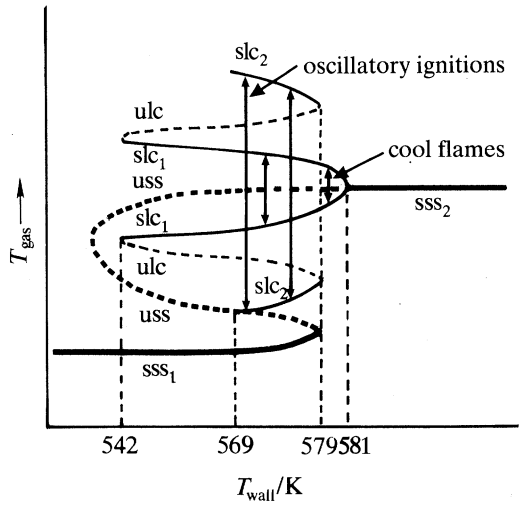

Figure 6. T_{gas}–T_{wall} bifurcation diagram. The stationary state locus is folded into an S-shaped hysteresis loop. The stable low reaction state, sss_1, exists for $T_{wall} \leqslant 579$ K. The high reaction state, sss_2, is stable at higher temperatures, but loses stability (uss) for $T_{wall} < 581$ K at a superficial Hopf bifurcation, giving birth to a small amplitude, stable limit cycle, slc_1, corresponding to cool flame oscillations. This limit cycle is lost at $T_{wall} = 542$ K when it merges with the unstable limit cycle ulc. There is a second stable limit cycle, slc_2, corresponding to the large amplitude, oscillatory ignitions for $T_{wall} \leqslant 579$ K, which terminate at $T_{wall} = 569$ K at a homoclinic orbit with the unstable, saddle point branch uss. ———, stable state; – – –, unstable state.

flame region occurs; alternatively a perturbation (sudden cooling) of the oscillatory cool flame system at temperatures below 579 K also gives access to the high-amplitude limit cycle. In each case, the ignitions are extinguished at $T_{wall} = 569$ K.

The major features, in particular the onset of oscillatory ignitions of a characteristic shape (a sharp ignition followed by a lower temperature tail), the transition to oscillatory cool flames and then to a high-temperature stationary state via a supercritical Hopf bifurcation, have been reproduced in detail modelling studies in a parallel investigation (Proudler *et al.* 1991). It is appropriate to outline the main results here.

The mechanism of the oxidation of alkanes in this low-temperature region is based on the alkylperoxy radical isomerization theory originally proposed by Fish (1968) and developed by Halstead *et al.* (1975, 1979) and by Cox (Cox & Cole 1985; Cox 1987). The mechanism involves the formation of a peroxy radical, RO_2, by reaction of an alkyl radical with O_2, and its isomerization by internal hydrogen abstraction to an alkylhydroperoxy radical. Subsequent reaction of this radical with O_2 followed by decomposition of the resulting peroxyhydroperoxy radical leads to the degenerate branching agents necessary for ignition.

The crucial aspects of the mechanism in the case of butane may be illustrated by reference to the *n*-butyl radical, formed by reaction of OH with *n*-butane:

$$OH + C_4H_{10} \rightarrow 1\text{-}C_4H_9 + H_2O\,, \qquad [1]$$

A related sequence of reactions also occurs via the $2\text{-}C_4H_9$ radical. The $1\text{-}C_4H_9$ radical reacts with O_2, forming the peroxy radical:

$$1\text{-}C_4H_9 + O_2 \rightleftharpoons 1\text{-}C_4H_9O_2\,, \qquad [2, -2]$$

which can then react to give degenerate branching agents via the hydroperoxy radical.

Branching accelerates the rate of reaction and of heat release thus increasing the temperature and leading to ignition. As the temperature increases, reaction [2] reverses and decomposition becomes the preferred route for consumption of $1\text{-}C_4H_9$:

$$1\text{-}C_4H_9 \rightarrow C_2H_5 + C_2H_4 \qquad [3]$$

This change of mechanism cuts off the main route to branching agents and the temperature falls. The ethyl radical generated in reaction [3] can itself lead to degenerate branching agents via the peroxy–hydroperoxy radical route, albeit with a lower rate of heat release; it is this weaker branching route that is responsible for the characteristic tail in the ignition profile.

As the background gas temperature increases, the concentration of $1\text{-}C_4H_9$ eventually exceeds that of $1\text{-}C_4H_9O_2$ even at this background temperature. The propensity of the system to generate branching agents is, in consequence, reduced as are the temperature excursions. The perturbation of the system by the heat release is considerably reduced and the model now generates sinusoidal rather than relaxation oscillations, in agreement with experiment.

Details of the mechanism, which is based on that of Cox & Olsson (1991), and a discussion of the numerical results will be published elsewhere (Proudler *et al.* 1991).

We are grateful to Dr S. K. Scott for helpful and illuminating discussions and to AEA Technology for a studentship (to V.K.P.).

References

Bardwell, J. 1954 Cool flames in butane oxidation. In *Proc. Fifth Symp. (Int) on Combustion*, pp. 529–534. Pittsburg, Pennsylvania: The Combustion Institute.

Baulch, D. L., Griffiths, J. F., Johnson, B. & Richter, R. 1990 Hydroxyl radical concentrations and reactant temperature profiles during oscillatory ignition of hydrogen: experimental measurements by laser resonance absorption spectroscopy and comparisons with numerical calculations. *Proc. R. Soc. Lond.* A **430**, 151–166.

Baulch, D. L., Griffiths, J. F., Kordylewski, W. & Richter, R. 1991 Experimental studies of the oscillatory combustion of hydrogen in a stirred flow reactor. *Phil. Trans. R. Soc. Lond.* A **337**, 199–210. (This volume.)

Bush, S. F. 1969 Design and operation of single-phase, jet-stirred reactors for chemical kinetic studies. *Trans. Int. Chem. Engng* **47**, T59–T72.

Caprio, V., Insola, A. & Lignola, P. G. 1976 Isobutane cool flames investigation in a continuous stirred tank reactor. In *Proc. 16th Symp. (Int.) on Combustion*, pp. 1155–1163. Pittsburg, Pennsylvania: The Combustion Institute.

Caprio, V., Insola, A. & Lignola, P. G. 1981 Isobutane cool flames in a CSTR: The behaviour dependence on temperature and residence time. *Combust. Flame* **43**, 23–33.

Caprio, V., Insola, A. & Lignola, P. G. 1983 *n*-Butane cool flames in a CSTR: The phenomenology dependence on temperature and residence time. *Archivum Combustionis* **3**, 27–38.

Cox, R. A. & Cole, J. A. 1985 Chemical aspects of the autoignition of hydrocarbon-air mixture. *Combust. Flame* **60**, 109–123.

Cox, R. A. 1987 Oxidation mechanisms in combustion systems. In *Modern gas kinetics* (ed. M. J. Pilling & I. W. M. Smith), pp. 262–283. Oxford: Blackwells.

Ferrer, M., David, R. & Millermaux, J. 1983 Homogeneous oxidation of *n*-butane in a self-stirred reactor, *Oxidat. Commun.* **4**, 353–368.

Fish, A. 1969 The non-isothermal oxidation of neopentane. *Combust. Flame* **13**, 23–32.

Franck, J., Griffiths, J. F. & Nimmo, W. 1986 In *Proc. 21st Symp. (Int.) on Combustion*, p. 447. Pittsburg, Pennsylvania: The Combustion Institute.

Gray, P. & Scott, S. K. 1990 *Chemical oscillations and instabilities*; *nonlinear chemical kinetics*. Oxford: Clarendon Press.

Griffiths, J. F. 1986 The fundamentals of spontaneous ignition of gaseous hydrocarbons and related organic compounds. *Adv. chem. Phys.* **64**, 203–303.

Griffiths, J. F., Nimmo, W., Franck, J. & Yahia, A. A. 1988 Fundamentals of autoignition in reciprocating engines. *Proc. Instn Mech. Engrs* **I**, 25–30.

Halstead, M. P., Kirsch, L. J., Prothero, A. & Quinn, C. P. 1975 Mathematical model for hydrocarbon autoignition at high pressures. *Proc. R. Soc. Lond.* A **346**, 515–538.

Halstead, M. P., Kirsch, L. J. & Quinn, C. P. 1977 The autoignition of hydrocarbon fuels at high temperatures and pressures – fitting a mathematical model. *Combust. Flame* **30**, 45.

Neu, J. T. 1956 Infrared spectrographic studies of preflame reactions of *n*-butane. *J. phys. Chem.* **60**, 320–324.

Malherbe, F. E. & Walsh, A. D. 1950 Experiments with cool frames. II. Pressure-temperature limits. *Trans. Faraday Soc.* **46**, 835–848.

Olson, G. & Cox, R. A. 1991 High pressure autoignition of butane, a chemical modelling study. *Combust. Flame*. (In the press.)

Proudler, V. K., Hughes, K. J. & Pilling, M. J. 1991 Modelling of thermokinetic processes for *n*-butane in a jet-stirred reactor. *Combust. Flame*. (In preparation.)

Pugh, S. A., Kim, H. R. & Ross, J. 1987 Measurements of [OH] and [CH_3CHO] oscillations and phase relations in the combustion of CH_3CHO. *J. chem. Phys.* **86**, 776–783.

PHILOSOPHICAL TRANSACTIONS OF THE ROYAL SOCIETY A MATHEMATICAL, PHYSICAL & ENGINEERING SCIENCES